

## Electronic Supplementary Information: 2D heavy fermion CePb<sub>3</sub> kagome material on silicon: Emergence of unique spin polarized states for spintronics

A.N. Mihalyuk,<sup>1,2,\*</sup> D.V. Gruznev,<sup>2</sup> L.V. Bondarenko,<sup>2</sup> A.Y. Tupchaya,<sup>2</sup>

Y.E. Vekovshinin,<sup>2</sup> S.V. Ereemeev,<sup>3</sup> A.V. Zotov,<sup>2</sup> and A.A. Saranin<sup>2</sup>

<sup>1</sup>*Institute of High Technologies and Advanced Materials,*

*Far Eastern Federal University, 690950 Vladivostok, Russia*

<sup>2</sup>*Institute of Automation and Control Processes FEB RAS, 690041 Vladivostok, Russia*

<sup>3</sup>*Institute of Strength Physics and Materials Science, Tomsk 634055, Russia*

### Formation processes of the Si(111) $\sqrt{3} \times \sqrt{3}$ -(Pb, Ce) surface

For the formation of the (Pb, Ce)/Si(111) system, we employed two procedures those differ in element deposition order and hence the initial surface. In the first procedure (Fig. S1 (a)), the initial surface was Si(111)1 $\times$ 1-Pb reconstruction, which comprises Pb monolayer residing on the bulk-like Si substrate. Fig. S2 (a) shows STM images of this surface prepared by 1 ML Pb deposition held at about 200°C. The images confirm high crystal quality of the surface with 1 $\times$ 1 lattice and low density of defects.

Room temperature (RT) deposition of Ce onto the Si(111)1 $\times$ 1-Pb surface leads to the formation of fractal nano-islands (Fig. S2 (b)). The initial Pb/Si(111) surface gains a lot of defects withal.

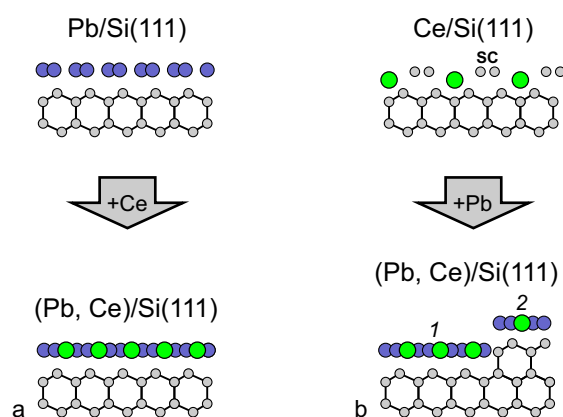


FIG. S1. Schematic representation of two procedures for the formation of the  $\sqrt{3} \times \sqrt{3}$ -(Pb, Ce)/Si(111) system. (a) Ce deposition onto Pb/Si(111) monolayer and (b) Pb adsorption onto Ce-induced surface reconstruction. “SC” stands for a Seiwatz chain, 1 and 2 indicate sub-terraces of the Si(111) substrate.

\* mih-alexey@yandex.ru

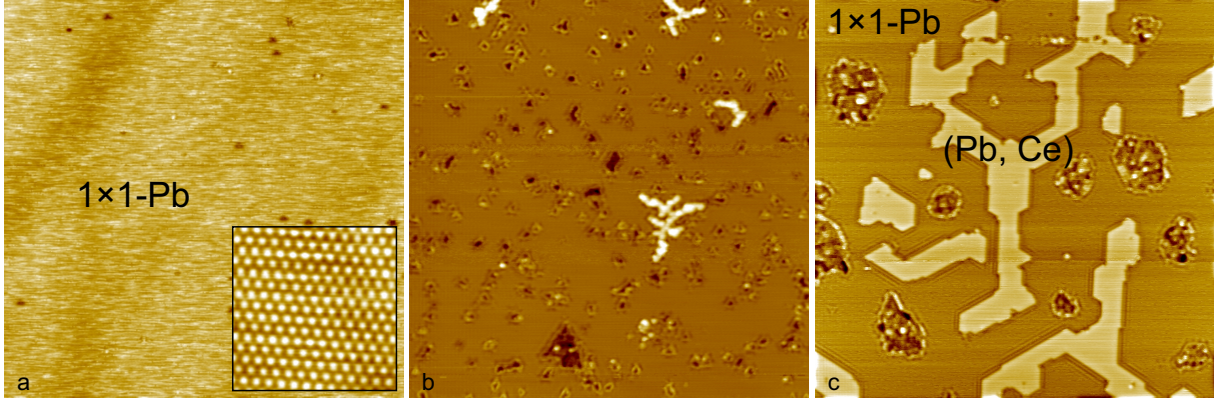


FIG. S2. Formation of the  $\sqrt{3} \times \sqrt{3}$ -(Pb, Ce) structure by the first procedure. (a) STM image ( $100 \times 100 \text{ nm}^2$ ) of the initial Si(111)1 $\times$ 1-Pb surface. Inset shows high resolution image ( $5 \times 5 \text{ nm}^2$ ). (b) STM image ( $100 \times 100 \text{ nm}^2$ ) recorded after  $\sim 0.1$  ML Ce deposition at room temperature. (c) STM image ( $100 \times 100 \text{ nm}^2$ ) of the same surface after short annealing at about  $400^\circ\text{C}$ .

Upon brief (few seconds) annealing at about  $400^\circ\text{C}$ , the interaction between Ce and Pb atoms takes place resulting in the formation of compound (Pb, Ce) layer (Fig. S2 (c)). Juggling from the absence of any noticeable Si mass transport, we concluded that the structure of the Si substrate beneath the layer remains unreconstructed. At the same time, the point defects agglomerate into huge patches of disordered surface. We attribute this to Pb desorption because of a relatively high temperature for the Pb/Si(111) system, and possibly to the initial stages of Ce-silicide formation.

Changing the order of Ce and Pb deposition slightly improves the quality of the final (Pb, Ce)/Si(111) surface. In this procedure, Ce-induced sub-monolayer reconstruction was prepared prior to Pb deposition (Fig. S1 (b)). In contrast to the Pb/Si(111) case, the Ce/Si(111) surface involves a fractional (comparing to a bulk-like Si bilayer) coverage of Si atoms. The extra Si atoms are incorporated in all lanthanide-induced reconstructions as additional Seiwatz and honeycomb chains [1, 2] as schematically shown in Fig. S1 (b). Fig. S3 (a) shows STM image and LEED pattern of the quasi-one-dimensional Si(111)3 $\times$ 2-Ce reconstruction prepared by  $1/3$  ML Ce deposition at  $\sim 800^\circ\text{C}$ . In this reconstruction, only Seiwatz chains of Si are present separated by rows of Ce atoms [2]. 1 ML Pb deposition on this surface at RT followed by annealing at about  $400^\circ\text{C}$  results in the formation of the same  $\sqrt{3} \times \sqrt{3}$ -(Pb, Ce) surface as in the previous case. However, fractional Si coverage of the initial Ce/Si(111) reconstruction have a consequence of splitting the terraces of Si(111) substrate in two sub-terraces marked in Figs. S1 (b) and S3 (b) by numbers “1” and “2” during decomposition of the initial Ce/Si(111) and formation of the  $\sqrt{3} \times \sqrt{3}$ -(Pb, Ce) reconstruction. STM images and LEED patterns (Fig. S3 (b)) confirm high crystal quality

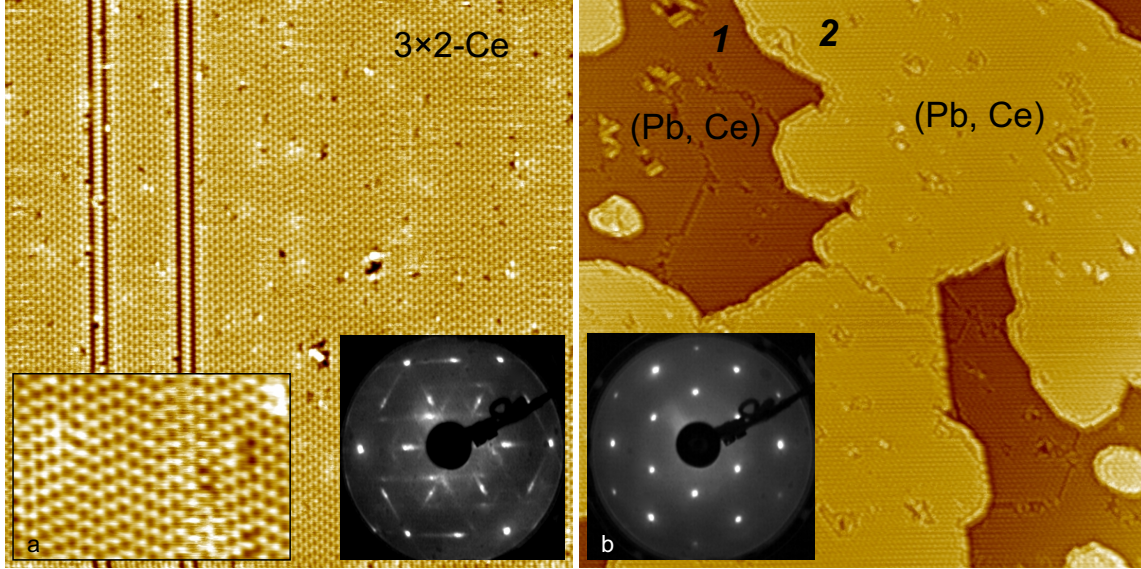


FIG. S3. Formation of the  $\sqrt{3} \times \sqrt{3}$ -(Pb, Ce) structure by the second procedure. (a) STM image ( $75 \times 75 \text{ nm}^2$ ) of the initial Si(111) $3 \times 2$ -Ce reconstruction. Insets show high resolution image ( $15 \times 10 \text{ nm}^2$ ) and LEED pattern (42 eV). (b) STM image ( $75 \times 75 \text{ nm}^2$ ) taken after 1 ML Pb deposition at RT followed by annealing at about  $400^\circ\text{C}$ . Inset shows LEED pattern (48 eV). *1* and *2* indicate sub-terraces of the Si(111) substrate.

and relatively low density of defects of the final surface. The  $\sqrt{3} \times \sqrt{3}$ -(Pb, Ce) surface is more thermally stable comparing to Si(111) $1 \times 1$ -Pb reconstruction (but not to the Si(111) $3 \times 2$ -Ce), i.e. its decomposition and desorption of Pb atoms takes place at higher temperatures. This indicates to stronger Pb – Ce bonding comparing to Pb – Si.

- 
- [1] M. Goshtasbi Rad, M. Göthelid, B. Hirschauer, and U. Karlsson, Applied Surface Science **166**, 209 (2000).
- [2] L. Liu, Z. Lin, Y. Wang, W. Wang, F. Yang, X. Zhu, and J. Guo, Surface Science **674**, 40 (2018).